

## Electrodeposition of Cu<sub>2</sub>O Nanopyramids Using an Anodic Aluminum Oxide Template

Chihiro Iida<sup>1</sup>, Miyu Sato<sup>1</sup>, Masaharu Nakayama<sup>1,\*</sup>, Atsushi Sanada<sup>2</sup>

<sup>1</sup> Materials Chemistry, Graduate School of Science and Engineering, Yamaguchi University, 2-16-1 Tokiwadai, Ube 755-8611, Japan

<sup>2</sup> Applied Physics, Graduate School of Science and Engineering, Yamaguchi University, 2-16-1 Tokiwadai, Ube 755-8611, Japan

\*E-mail: [nkymm@yamaguchi-u.ac.jp](mailto:nkymm@yamaguchi-u.ac.jp)

Received: 26 July 2011 / Accepted: 2 September 2011 / Published: 1 October 2011

---

Application of repetitive potential pulses to the anodic aluminum oxide (AAO) template on an Al substrate in an acid electrolyte containing Cu<sup>2+</sup> ions led to the formation of cupric oxide (Cu<sub>2</sub>O) on the AAO surface. The deposited Cu<sub>2</sub>O particles were not of octahedral crystals oriented randomly but of pyramidal shape having a strongly preferred orientation in the {100} direction. The pyramids were rooted in the AAO cylindrical pores, which evidences a growth mechanism in which a certain number of Cu<sub>2</sub>O deposits that overflow simultaneously from the pores grow to connect with each other to build a cluster of pyramidal shape.

---

**Keywords:** electrodeposition, Cu<sub>2</sub>O, nanopyramids, orientation, SIM

### 1. INTRODUCTION

Cupric oxide (Cu<sub>2</sub>O) is a well-known p-type semiconductor with a direct band gap energy of 2 eV, which makes it a promising material for converting solar energy into electrical or chemical energy. A variety of methods have been used in attempts to deposit thin films of Cu<sub>2</sub>O, including thermal oxidation of a metallic copper sheet [1], chemical deposition [2], reactive magnetron sputtering [3], pulsed laser deposition [4], plasma evaporation [5] and electrodeposition [6]. Electrodeposition is an attractive route for the production of metal oxide films because the thickness, composition, crystal structure, and morphology can be controlled by adjusting electrochemical parameters even on a substrate of complex shape [7].

The energy conversion efficiency of a solar cell is related to morphology as well as their band gap [8]. Cu<sub>2</sub>O crystals with various morphologies have been prepared electrochemically with the

addition of surfactants [9] or under the control of current density [10], temperature [10], pH [9], and microstructure of substrate [11]. However, the fabrication of nanocrystals with high symmetry such as tetrahedron, cube, octahedron, dodecahedron, and icosahedron is still a major challenge [12]. Moreover, control of the crystal orientation is worth revealing because differently oriented  $\text{Cu}_2\text{O}$  films provide different values of flatband potential [13].

On the other hand, anodic alumina oxide (AAO) has a hexagonally packed array of highly ordered cylindrical pores, which is formed by anodic oxidation of pure aluminum [14]. Electrodeposition of metals or metal oxides using patterned AAO as a template has received considerable attention with the aim of fabrication of nanostructures because of several advantages such as simplicity, cost effectiveness, and the possibility of large-area production [15-17]. Although the formation of  $\text{Cu}_2\text{O}$  crystals by electrodeposition have been intensively investigated, to the best of our knowledge, the formation of well-defined  $\text{Cu}_2\text{O}$  crystals with a strong preferred orientation from an acidic bath has never been reported. In the present study, we electrodeposited  $\text{Cu}_2\text{O}$  nanopyramids through an AAO template that was kept on Al substrate, where the barrier layer at the bottom of AAO pores was thinned to improve the electrical conductivity. The products were characterized by x-ray diffraction (XRD) and imaged by field emission scanning electron microscopy (FE-SEM) and scanning ion microscopy (SIM).

## 2. EXPERIMENTAL

Anodic oxidation was carried out in a two-electrode cell, equipped with an aluminum foil as the counter electrode. High purity (99.999 %, Nilaco) plain aluminum foil was used as a starting material. A highly ordered AAO template was prepared by a conventional two-step anodic process [14]. The first anodization was performed in 0.3 M  $(\text{COOH})_2$  solution by a constant voltage of 50 V at 0 °C for 3h. The surface oxide layer formed during the anodization was removed in an aqueous solution containing 0.5 M  $\text{H}_3\text{PO}_4$  and 0.2 M  $\text{CrO}_3$  at 80 °C. Then, the anodization was made again under the same conditions for 25 min. After the second step, the barrier layer was thinned and eventually removed to offer a better condition for the subsequent electrodeposition. We confirmed that the AAO template thus obtained consisted of highly ordered hexagonally packed cylindrical pores of about 100 nm in diameter, by FE-SEM.

The AAO template kept on Al foil served as the working electrode. A platinum sheet and an Ag/AgCl electrode were used as the auxiliary and reference electrodes, respectively. Electrodeposition was performed at 25 °C in a solution containing 0.2 M  $\text{CuSO}_4$  and 0.8 M  $\text{H}_3\text{BO}_3$  by applying repetitive potential pulses at a frequency of 50 Hz. The obtained deposits were characterized using XRD, FE-SEM, and SIM techniques. XRD patterns were recorded using a Rigaku diffractometer with  $\text{Cu K}_\alpha$  radiation ( $\lambda=0.15405$  nm). For identification, JCPDS Cards no. 05-0667 ( $\text{Cu}_2\text{O}$ ) and 04-0836 (Cu) were used. FE-SEM data were obtained with a Hitachi S-4700Y scanning electron microscopy. SIM images of the FIB-processed samples were acquired using a Hitachi FB2200 focused ion beam system.

### 3. RESULTS AND DISCUSSION

Fig. 1 shows XRD patterns of the AAO/Al substrate with a pore diameter of 100 nm (hereafter, designated as AAO<sub>100</sub>), taken after applying square wave potential pulses in a solution containing 0.2 M CuSO<sub>4</sub> and 0.8 M H<sub>3</sub>BO<sub>3</sub>. The combinations of anodic/cathodic potentials were +8/-10 (a), +8/-8 (b), and +10/-8 V (c). Two peaks appearing at 43.3° and 50.5° can be indexed to the 111 and 200 crystal planes of metallic copper (JCPDS04-0836). The peaks at 36.4°, 42.3°, and 61.3° can be attributed to the 111, 200, and 220 crystal planes of Cu<sub>2</sub>O with cubic symmetry, respectively (JCPDS05-0667). As seen from pattern b, the potential pulses between +8 and -8 V give rise to a mixture of Cu and Cu<sub>2</sub>O, while pure Cu and Cu<sub>2</sub>O phases are observed in pattern a and c, respectively. Namely, pure Cu and Cu<sub>2</sub>O crystals can be obtained selectively from the same solution when the applied potential was shifted more negative (a) and positive (c), respectively. This suggests that Cu is formed during the cathodic step (1), which is followed by reoxidation to Cu<sub>2</sub>O during the anodic step (2):

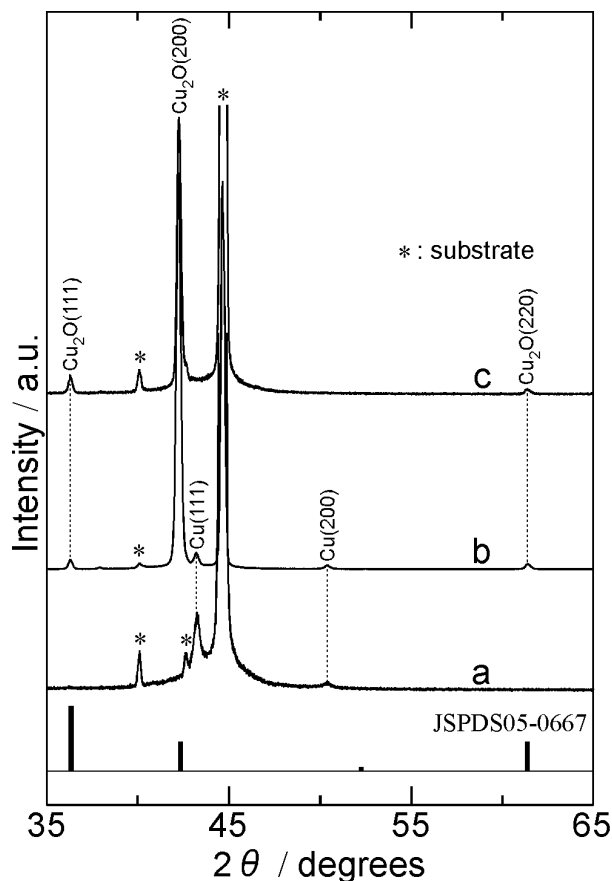


**Figure 1.** XRD patterns of the AAO<sub>100</sub>/Al electrode obtained after applying potential pulses between (a) +8 and -10, (b) +8 and -8, (c) +10 and -8 V in a 0.2 M CuSO<sub>4</sub> and 0.8 M H<sub>3</sub>BO<sub>3</sub> solution.

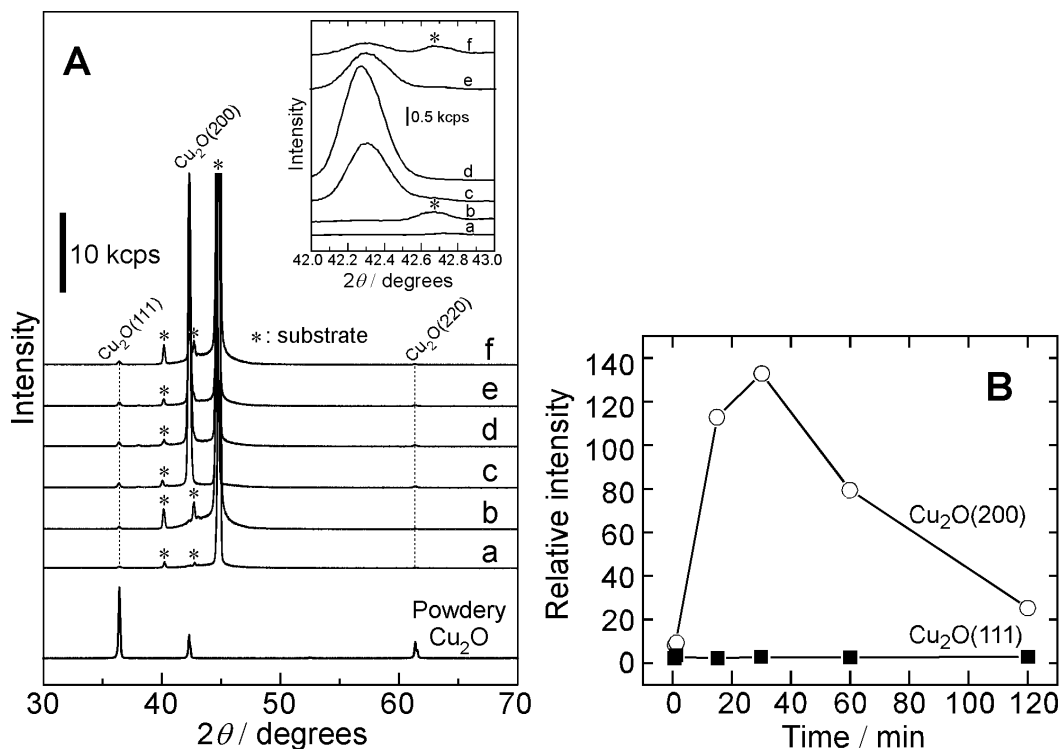


**Figure 2.** (A) XRD patterns of  $\text{Cu}_2\text{O}$  crystals deposited on the  $\text{AAO}_{100}/\text{Al}$  electrode, by applying potential pulses of +10/-8 V for (a) 0.5, (b) 1, (c) 15, (d) 30, (e) 60, and (f) 120 min. The deposition bath contained 0.2 M  $\text{CuSO}_4$  and 0.8 M  $\text{H}_3\text{BO}_3$ . (B) Plots of the relative intensities of the 200 (○) and 111 (■) peaks to the intensity of the 220 peak as a function of deposition time.

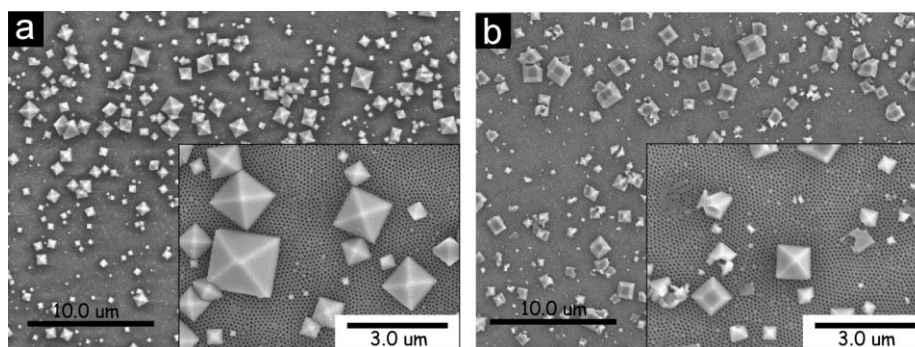


**Figure 3.** SEM images of the  $\text{Cu}_2\text{O}$  crystals deposited on the  $\text{AAO}_{100}/\text{Al}$  electrode by applying potential pulses of +10/-8 V for (a) 15 and (b) 60 min.

Fig. 2A displays XRD patterns of the  $\text{Cu}_2\text{O}$  crystals deposited on the  $\text{AAO}_{100}/\text{Al}$  electrode by applying potential pulses between +10 and -8 V for different periods of time. It is confirmed that the crystal structure itself is independent of the deposition time. As also shown in the inset, the relative intensity of the 200 peak is much larger than that of bulk  $\text{Cu}_2\text{O}$  or the JCPDS data. This demonstrates that the deposited  $\text{Cu}_2\text{O}$  has a strong {100} preferred orientation. The relative intensities of the 200 and 111 with respect to the 220 peak are plotted in Fig. 2B as a function of deposition time. The intensity

of the 200 peak increases with deposition time to reach a maximum at 30 min and then decreases, while the 111 peak remains almost constant in intensity.

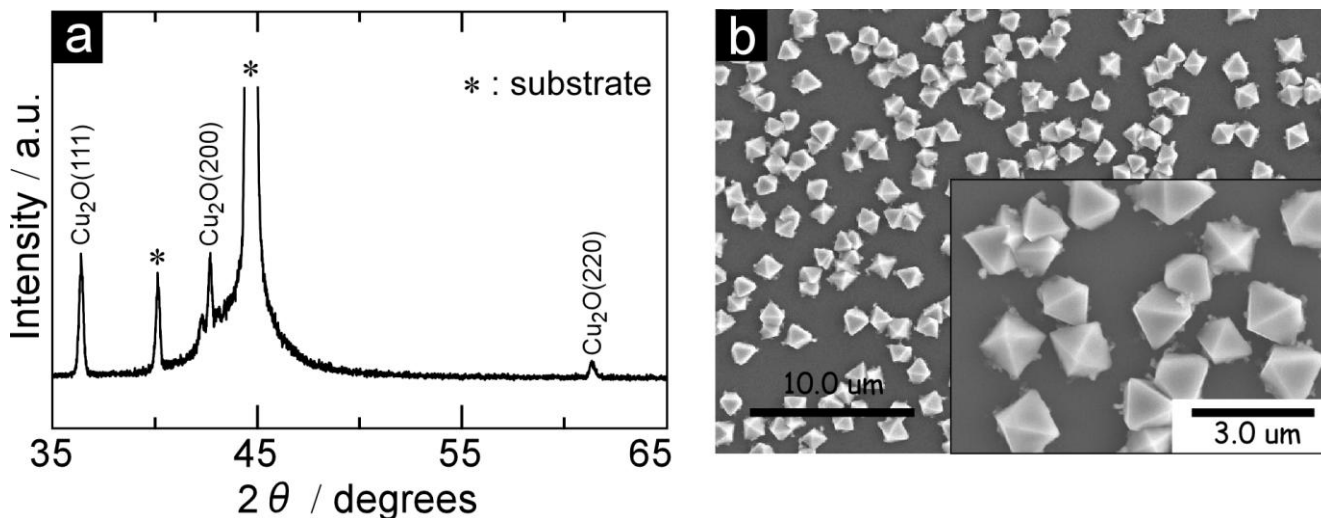


**Figure 4.** (a) XRD and (b) SEM data of a plain Al electrode taken after applying potential pulses between +10 and -8 V in a solution containing 0.2 M  $\text{CuSO}_4$  and 0.8 M  $\text{H}_3\text{BO}_3$ .

Fig. 4 shows XRD (a) and SEM (b) data taken when the same electrodeposition was conducted on a plain Al foil to deposit  $\text{Cu}_2\text{O}$ . The resulting Al electrode no longer provides the enhanced 200 peak. Rather, the pattern is similar to that (Fig. 2A) of bulk  $\text{Cu}_2\text{O}$  from the point of view that the relative intensity of the 111 plane is strongest. In fact, the SEM photograph presents octahedral  $\text{Cu}_2\text{O}$  particles with a size of about 1  $\mu\text{m}$ , most of which expose their 111 planes.

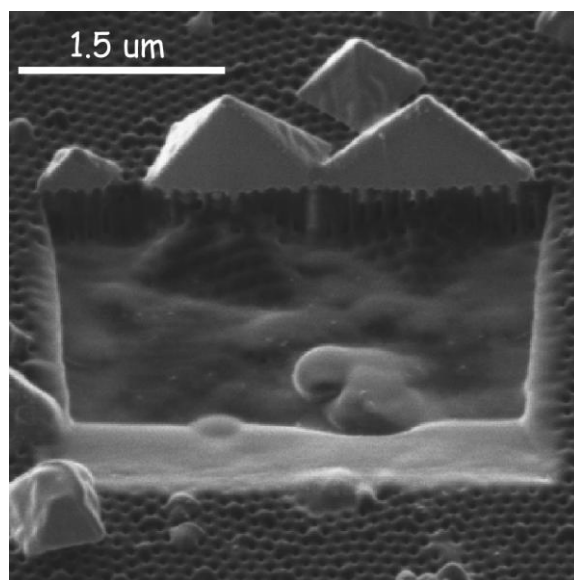


**Figure 5.** SIM image of the surface  $\text{AAO}_{100}/\text{Al}$  electrode prepared in Fig. 3a.

Fig. 3 shows SEM photographs of the electrode surface after the deposition of  $\text{Cu}_2\text{O}$ . No deposits could be detected in the film with the deposition time of 1 min (not shown). As seen from Fig. 2A, there is no pronounced 200 peak within 1 min in XRD pattern, though the 111 peak is visible. This suggests that the growth of  $\text{Cu}_2\text{O}$  inside the cylindrical AAO pores is not a shape-guide process. This observation is different from that reported by Wang et al. where  $\text{Cu}_2\text{O}$  nanowires with a strong 200 reflection were grown inside the AAO pores from a  $\text{CuSO}_4$  solution of pH 5 [18]. In Fig. 3a, we can see a number of well-formed tetragonal pyramids with sizes ranging from 0.5 to 2.0  $\mu\text{m}$  over the whole substrate. Certainly, this structure has the {100} plane oriented parallel to the surface of  $\text{AAO}_{100}$ , which is in good agreement with the above XRD data. In the film prepared with the deposition time of 60 min (Fig. 3b), the collapse of the pyramidal crystals is obvious in both low and high magnification images, consistent with the observed decrease in the intensity of the 200 peak after 30 min. Although further investigation is now underway to derive a precise mechanism, the prolonged pulses may cause oxidative dissolution of the  $\text{Cu}_2\text{O}$  crystals.

Fig. 5 displays a SIM image of the surface of the  $\text{AAO}_{100}/\text{Al}$  electrode taken after the electrodeposition of  $\text{Cu}_2\text{O}$  crystals and then being shaved off by FIB. The obtained image evidences that the crystals are of pyramidal shape, and not of octahedral, and clearly indicates that the pyramids are rooted in the AAO pores and the cylindrical pores of AAO act as starting points in the crystal growth of  $\text{Cu}_2\text{O}$ . Probably, a certain number of  $\text{Cu}_2\text{O}$  deposits that overflow simultaneously from the AAO cylindrical pores grow to connect with each other to build a cluster of pyramidal shape.

#### 4. CONCLUSIONS

Application of pulsed potentials to an AAO template/Al substrate in acid solution with  $\text{Cu}^{2+}$  ions provided pyramidal  $\text{Cu}_2\text{O}$  crystals with a strong {100} preferred orientation, judging from the pronounced 200 diffraction. The pyramids were rooted in the cylindrical pores of AAO, which may reflect that  $\text{Cu}_2\text{O}$  deposits overflowing from the pores aggregate to build a cluster of pyramidal shape.

#### ACKNOWLEDGEMENT

This work was supported by a Grant-in-Aid for Scientific Research on Innovation Areas "Electromagnetic Metamaterials" (No. 23109510) of The Ministry of Education, Culture, Sports, and Technology, Japan.

#### References

1. A. O. Musa, T. Akomolafe, M. J. Carter, *Sol. Energy Mater. Sol. Cells*. 51 (1998) 305.
2. Y. Hameş, S. E. San, *Sol. Energy*. 77 (2004) 291.
3. S. Ishizuka, T. Maruyama, K. Akimoto, *Jpn. J. Appl. Phys.* 39 (2000) L786.
4. M. Ivill, M. E. Overberg, C. R. Abernathy, D. P. Norton, A. F. Hebard, N. Theodoropoulou, J. D. Budai, *Solid-State Electron*. 47 (2003) 2215.
5. K. Santra, C. K. Sarkar, M. K. Mukherjee, B. Ghosh, *Thin Solid Films* 213 (1992) 226.
6. M. Nakayama, S. Konishi, H. Tagashira, K. Ogura, *Langmuir* 21 (2005) 354.

7. P. E. de Jongh, D. Vanmaekelbergh, J. J. Kelly, *Chem. Mater.* 11 (1999) 3512.
8. K. E. R. Brown, K.-S. Choi, *Chem. Commun.* (2006) 3311.
9. M. J. Siegfried, K.-S. Choi, *Adv. Mater.* 16 (2004) 1743.
10. M. J. Siegfried, K.-S. Choi, *Angew. Chem., Int. Ed.* 44 (2005) 3218.
11. J. K. Barton, A. A. Vertegel, E. W. Bohannon, J. A. Switzer, *Chem. Mater.* 13 (2001) 952.
12. S. Guo, Y. Fang, S. Dong, E. Wang, *Inorg. Chem.* 46 (2007) 9537.
13. L. C. Wang, N. R. de Tacconi, C. R. Chenthanmarakshan, K. Rajeshwar, M. Tao, *Thin Solid Films* 515 (2007) 3090.
14. H. Masuda, M. Satoh, *Jpn. J. Appl. Phys.* 35 (1996) L126.
15. F. Cheng, H. Wang, Z. Sun, M. Ning, Z. Cai, M. Zhang, *Electrochem. Commun.* 10 (2008) 798.
16. T. Chowdhury, D. P. Casey, J. F. Rohan, *Electrochem. Commun.* 11 (2009) 1203.
17. C.-L. Xu, S.-J. Bao, L.-B. Kong, H. Li, H.-L. Li, *J. Solid State Chem.* 179 (2006) 1351.
18. X. Wang, C. Li, G. Chen, L. He, H. Cao, B. Zhang, *Solid State Sci.* 13 (2011) 280.